

Physical Optics Analysis of a Four-Reflector Antenna Part 1

A. G. Cha

Radio Frequency and Microwave Subsystems Section

Concern has been raised for the 64-m to 70-m antenna upgrade project that the 70-m system may experience greater S-band beam-pointing perturbations than the 64-m system. The S-band perturbations are due to minor (higher order) mode generation, causing subtle cross-polarization fields affecting beam pointing direction, as described herein. For the antennas in their present configuration (64 m), a slight S-band gain degradation of about 0.05 dB can be attributed to these effects. Therefore, a full physical optics analysis was performed for the present-day 64-m system, as described herein. The results were compared with past analyses and experimental observations in order to verify the algebra and computer code with the intent of deriving a valid analysis method for accurately analyzing the 70-m shaped dual-reflector Cassegrainian antenna. The results of the new analysis appear to be in excellent agreement with previous analyses and experimental data, and extension of the analysis methods to the 70-m system will follow in a second article.

I. Introduction

In support of the DSN 64-m to 70-m antenna upgrade project, several RF performance analyses were made based on a two-reflector, linearly polarized antenna system at X-band and S-band. However, the two-reflector analysis is valid only at X-band. At S-band, the antenna (64-m or 70-m) is in reality a four-reflector system. The present-day DSN 64-m antennas use conventional paraboloidal and hyperboloidal Cassegrainian reflectors, with the hyperboloidal subreflector modified in three major ways. First, the vertex is displaced from the main reflector centerline such that a line connects the main reflector focal point, the subreflector vertex, and the primary feedhorn phase center. Second, the subreflector rim is trimmed to describe a cone of $2\Theta = 120^\circ$, centered on the main reflector axis of symmetry. Lastly, a special spillover-reducing conical flange is used around the periphery of the offset and asymmetrically trimmed hyperboloid. The overall antenna system

employs two additional S-band reflectors near the primary feeds, one ellipsoidal and the other planar, to make up a four-reflector antenna at S-band. These reflectors, which enable simultaneous S- and X-band use of the overall antenna (S-band uplink and downlink and X-band downlink), complicate the analyses because of the close proximity to geometric optics focal points (see Fig. 1).

The 70-m Cassegrainian subreflector is specially shaped for uniform amplitude illumination of the primary reflector and is slightly asymmetric in order to accommodate offset primary feeds. Two additional reflectors in the primary feed region are also used in the same manner mentioned above for the 64-m antenna.

Neither reflector in the primary feed region can be analyzed using simple geometric optics or usual far-field ap-

proaches. Figure 2 shows the complex physics involved, i.e., the divergence and bunching of the RF energy beam as computed from a near-field analysis. Furthermore, the necessary physical asymmetries involved in these multi-function antenna instruments cause second-order (but important) perturbations in the final aperture beam directions when circular polarization is used. The beam-direction perturbation can be predicted only in a four-reflector antenna analysis that also takes into account near-field and circular polarization effects.

It was necessary to use some approximations in the previous analyses of the present-day system. For example, only a rough analysis of final aperture beam directions was made. Concern exists that the 70-m system, which effectively illuminates the main reflector in a uniform way, may experience greater S-band perturbations or beam squints (i.e., non-coincident right circularly polarized/left circularly polarized beams) than the 64-m system. Accordingly, it was decided to first perform a full analysis of the existing 64-m S-band system, since previous experimental results are available for comparison (Ref. 1).

If the present analysis effort is verified by comparison with previous experiments, the work will be extended to include the 70-m shaped asymmetric subreflector and shaped symmetric main reflector. For a full analysis, the S-band horn fields will be carried through all four reflectors (resulting in a transmission viewpoint of final antenna system beams) to account fully for all near-field, cross-polarization, and higher order mode generation effects caused by various intentional asymmetries. This appears to be the first time such a complete and rigorous analysis has been performed on such a complex antenna system.

II. Background

A comprehensive description of the 64-m antenna S/X-band reflex feed system was presented by Bathker in 1974 (Ref. 1). An analysis of the observed 64-m antenna S-band beam position offset from antenna boresight was performed by the author in 1977 (Ref. 2). The analysis made use of a diffraction analysis (physical optics) of the feedhorn/ellipsoid/dichroic assembly performed by Potter (Ref. 3). The analysis by Potter was combined with a geometric-optics analysis of the hyperboloid scattering, and with an aperture field integration computation of the antenna secondary field, to predict the final antenna beam direction. While this early approach worked very well in the 64-m antenna case, the algebra and computer code developed were essentially limited to the hyperboloid/paraboloid case, and could not be easily extended to the 70-m dual-shaped reflector system.

The present analysis goes far beyond previous analyses in many ways. The analysis methods can be used for both hyperbolic/parabolic and dual-shaped reflectors. It is a true four-reflector, circular-polarization, near-field physical optics analysis. Figure 1 shows the four-reflector system, consisting of the S-band feedhorn the ellipsoid, the dichroic plate, the asymmetric subreflector, and the symmetric main reflector. Figure 3 shows a simplified block diagram of the analysis approach. Near-field diffraction patterns were computed using standard JPL spherical wave expansion (SWE) techniques developed by Ludwig. The far field of each subreflector is first found by use of conventional physical optics integrations. This is followed by a numerical expansion of the far field to obtain the spherical wave mode coefficients. Finally, near-field computations result from using these coefficients (Ref. 4).

III. Results

The observed RF beam positions of the 64-m antenna are shown in Fig. 4. There are two significant beam position offsets from the antenna boresight, as explained in Ref. 1. The 0.0114° offset (Fig. 4) of the X-band beam is due to the finite thickness of the dichroic plate, which causes a refraction effect as the X-band wave propagates through the dichroic plate. When this was found, the position of the dichroic plate was shimmed by 1 in. The shimming brought the S- and X-band beams together in the direction of center-to-center line of the S- and X-band feedhorns, as seen in Fig. 4. The S-band right circularly polarized beam has another offset of 0.0086° normal to this direction. This offset is attributed to the higher order ($m \neq 1$) modes generated at the ellipsoid and is predicted to be observable only for circularly polarized waves. Alternately, this offset can be considered as a depolarization effect caused by the asymmetric ellipsoid geometry.

The new numerical results are 90% in agreement with experimental results observed in Fig. 4. Beam offset of a right circularly polarized wave from the antenna boresight was previously measured at 0.0086° and computed to be 0.0095° (0.061 beamwidth measured; 0.068 beamwidth computed). (It is expected that the left circularly polarized wave offset would be 0.0086° in the opposite direction from the antenna boresight, although this was not measured.) Beam offset due to a 1-in. shim in the position of the dichroic was measured at 0.0114° and computed to be 0.010° (0.081 BW measured; 0.071 BW computed). Table 1 shows the computed beam offset caused by the 1-in. shim of the dichroic position. Table 2 shows the right circularly polarized beam offset from antenna boresight. Together, Tables 1 and 2 indicate that the S-band beam position will be offset by 0.010° and 0.0095° in the two mutually perpendicular directions.

In addition to good correlation with observed RF beam positions, the present analysis also yields a reflector gain computation that can be compared with previous efficiency computations. A gain of 62.66 dB, corresponding to an efficiency of 77.6%, was computed, including spillover losses, non-uniform illumination and phase, higher order mode ($m \neq 1$), and polarization losses. These losses were previously computed to be (Ref. 1):

$$\begin{aligned} \eta_{FS} &= -0.133 \text{ dB} \\ \eta_{RS} &= -0.010 \text{ dB} \\ \eta_I &= -0.84 \text{ dB} \\ \eta_p &= -0.07 \text{ dB} \\ \eta_x &= -0.005 \text{ dB} \\ \eta_{m \neq 1} &= -0.089 \text{ dB} \end{aligned}$$

The total losses computed previously (Ref. 1) were -1.147 dB (76.8%), compared to present computed losses of -1.10 dB (77.6%). An item-by-item loss comparison is not possible because the present gain computation does not provide a breakdown of individual loss components.

The only small uncertainty of the analysis is that the hyperboloid flange was not included. It is not believed this would make any difference in the beam position prediction. However, efficiency (gain) computation is affected. It is likely that the difference in the two efficiency computations is mostly due to the fact that the subreflector flange was modeled in the earlier analysis. Since future DSN systems will not use such flanges, no effort was expended patching this part of the model into the new software. The difference is less likely due to numerical inaccuracies of either computation.

The new capabilities developed with this work include (1) software for analyzing the arbitrary wave polarization case (linear, circular, and elliptic) at near-field distance (see Appendix A), and (2) a physical optics program for computing symmetric main reflector diffraction when illuminated by asymmetric feed radiation patterns in the form of spherical wave harmonics. These programs enhance physical optics analysis capability and will be useful in other analysis activities. They are applicable to ongoing ground station antenna research and development efforts such as beam waveguide feed systems, holographic data reduction, and verification of GTD analysis software. As stated, this appears to be the first time such a complete and rigorous analysis has been performed on such a complex antenna system. Future work will extend the present results to the planned DSN 70-m dual-shaped reflector system with reflex-dichroic feed.

Acknowledgment

Many helpful discussions on the reflex feed with D. A. Bathker and D. Nixon are acknowledged. The author also thanks P. W. Cramer for providing the SYM-SCAT program used to analyze the main reflector in the four-reflector analysis.

References

1. Bathker, D. A., "Dual-Frequency Dichroic Feed Performance," presented at 26th Meeting of Avioincs Panel, AGARD, Munich, Germany, November 26-30, 1973, *AGARD Conference Proceedings #139*, pp. 29-1-29-9, June 1974, NATO.
2. Cha, A. G., "Beam Squint in Large Ground Station Antennas," presented at International Antennas and Propagation Symposium, Stanford, California, 1977, *1977 International Symposium Digest, Antennas and Propagation*, pp. 538-541.
3. Potter, P. D., "S- and X-band RF Feed System," *JPL Technical Report 32-1526, Vol. III*, pp. 53-60. Jet Propulsion Laboratory, Pasadena, Calif., April 1972.
4. Ludwig, A. C., "Near-Field, Far-Field Transformations Using Spherical Wave Expansions," *IEEE Transactions on Antennas and Propagation*, March 1971, Vol. AP-19, pp. 214-220.

Table 1. Beam offset caused by 1-in. shim of dichroic position*

Theta	E Theta		E Phi		Axial Ratio	Ellipse Tilt Angle	RCP Gain, dB
	Volts	Phase	Volts	Phase			
0.00000	148.981325	-98.451	148.897799	171.534	0.005	166.91661	62.600
0.00100	149.165831	-98.443	149.075554	171.540	0.006	166.89899	62.610
0.00200	149.331051	-98.435	149.234343	171.547	0.006	166.85301	62.620
0.00300	149.476992	-98.426	149.374123	171.554	0.007	166.78256	62.628
0.00400	149.603628	-98.418	149.494875	171.561	0.007	166.69550	62.635
0.00500	149.710876	-98.409	149.596622	171.569	0.007	166.57938	62.641
0.00600	149.798769	-98.400	149.679274	171.576	0.008	166.45171	62.646
0.00700	149.867254	-98.392	149.742825	171.584	0.008	166.30922	62.650
0.00800	149.916344	-98.382	149.787300	171.592	0.008	166.14984	62.653
0.00900	149.945999	-98.373	149.812653	171.600	0.009	165.97935	62.654
0.01000**	149.956234	-98.363	149.818916	171.608	0.009	165.79265	62.655**
0.01100	149.947079	-98.354	149.806078	171.617	0.009	165.59603	62.654
0.01200	149.918497	-98.344	149.774174	171.625	0.010	165.38231	62.652
0.01300	149.870565	-98.334	149.723173	171.634	0.010	165.15844	62.650
0.01400	149.803247	-98.321	149.653156	171.646	0.010	164.92001	62.646
0.01500	149.716541	-98.310	149.564074	171.655	0.010	164.66658	62.640
0.01600	149.610556	-98.300	149.456049	171.665	0.010	164.39746	62.634
0.01700	149.485386	-98.288	149.329130	171.675	0.011	164.11704	62.627
0.01800	149.340899	-98.276	149.183241	171.685	0.011	163.81953	62.618
0.01900	149.177284	-98.265	149.018515	171.695	0.011	163.50879	62.609
0.02000	148.994564	-98.253	148.835079	171.706	0.011	163.17743	62.598

*Plane $\phi = 180^\circ$ (direction of 0.0114° beam offset, see Fig. 4).

**Beam position for peak gain.

Table 2. Offset of right circularly polarized beam from antenna boresight*

Theta	E Theta		E Phi		Axial Ratio	Ellipse Tilt Angle	RCP Gain, dB
	Volts	Phase	Volts	Phase			
0.00000	148.897789	171.534	148.981325	81.549	0.005	166.91653	62.600
0.00100	149.070080	171.480	149.155140	81.495	0.005	168.19427	62.610
0.00200	149.223063	171.427	149.309898	81.440	0.005	169.51804	62.619
0.00300	149.356670	171.375	149.445599	81.386	0.005	170.87561	62.627
0.00400	149.470888	171.323	149.562214	81.332	0.006	172.24525	62.633
0.00500	149.565687	171.271	149.659662	81.279	0.006	173.60888	62.639
0.00600	149.641045	171.219	149.737972	81.225	0.006	174.95147	62.643
0.00700	149.696924	171.167	149.797089	81.172	0.006	176.25542	62.647
0.00800	149.733271	171.116	149.836979	81.120	0.006	177.50557	62.649
0.00900**	149.750128	171.065	149.857647	81.067	0.006	178.69234	62.650**
0.01000**	149.747488	171.015	149.859093	81.015	0.006	179.81087	62.650**
0.01100	149.725349	170.964	149.841316	80.963	0.007	0.85489	62.649
0.01200	149.683687	170.914	149.804310	80.911	0.007	1.82267	62.646
0.01300	149.622532	170.864	149.748096	80.860	0.007	2.71287	62.643
0.01400	149.541880	170.817	149.672674	80.811	0.008	3.52796	62.639
0.01500	149.441759	170.768	149.578032	80.760	0.008	4.26989	62.633
0.01600	149.322292	170.719	149.464272	80.709	0.008	4.94688	62.626
0.01700	149.183455	170.671	149.331474	80.660	0.009	5.55535	62.618
0.01800	149.025164	170.623	149.179470	80.610	0.009	6.10518	62.609
0.01900	148.847649	170.574	149.008514	80.560	0.010	6.59810	62.599
0.02000	148.650909	170.526	148.818573	80.510	0.010	7.04187	62.588

*Plane $\phi = 270^\circ$ (direction of 0.0086° beam offset, see Fig. 4).

**Beam position for peak gain.

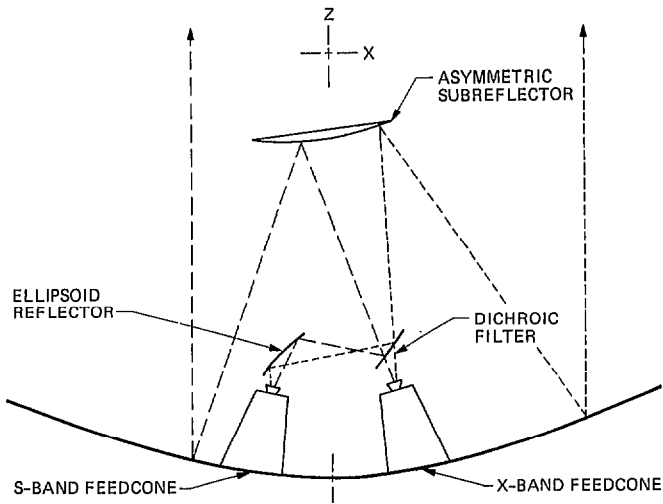


Fig. 1. The 64-m antenna four-reflector antenna system using S/X-band reflex dichroic feed

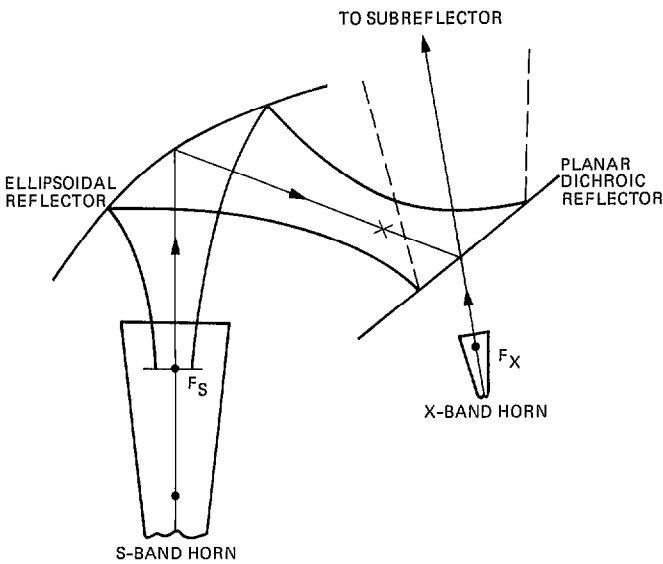


Fig. 2. Detail of reflex dichroic optics

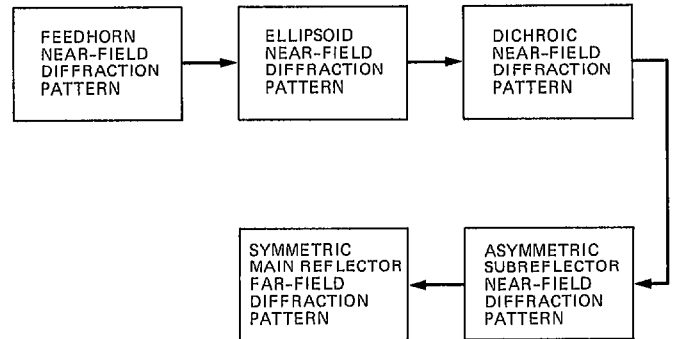


Fig. 3. Block diagram of physical optics analysis approach

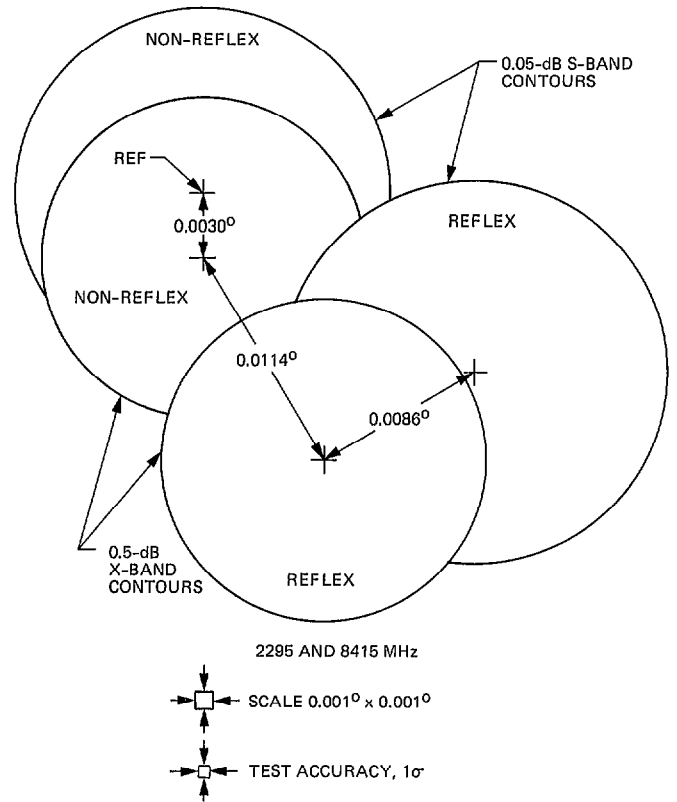


Fig. 4. Dual-frequency dichroic feed RF beam positions

Appendix A

Computer Program List

Program Name	Usage
HYBRIDHORN	Computes corrugated horn pattern and spherical wave coefficients for vertical (y) polarization.
YTXPOL/SWCOE	Obtains horn pattern spherical wave coefficient set for horizontal (x) polarization. Input is spherical wave coefficient set for y polarization.
YTORCP/SWCOE	Obtain horn pattern spherical wave coefficient set for RCP. Input is spherical coefficient wave set for y polarization.
FSCATT	Ludwig (Ref. 4) asymmetric reflector physical optics analysis program. Computes far-field diffraction patterns of ellipsoid, dichroic plate, and hyperboloid.
AZ-EXPAND-LG and SPW-ITER	Programs for computing spherical wave coefficient set of given (near- or far-field) pattern. Performed four times for ellipsoid, dichroic, and hyperboloid.
SYM-SCAT	Cramer symmetric reflector physical optics analysis program, used in computing far-field pattern of 64-m parabolic main reflector.
PHASE-CENT	Determines near-field phase center for given source (near- or far-field), pattern, and distance.
FGRID	Produces FSCATT integration grid for ellipsoid.
FSURF	Produces FSCATT surface definition for ellipsoid.
FGRIDPLT	Provides FSCATT integration grid for dichroic plate.
FSVRFPLT	Produces FSCATT surface definition for dichroic plate.